Journal of Nuclear Materials 195 (1992) 277–285
North-Holland

journal of nuclear materials

A ballistic mixing model for the amorphization of precipitates in Zircaloy under neutron irradiation

Arthur T. Motta [1] and Clément Lemaignan

CEA, DRN, SECC, Centre d'Etudes Nucléaires de Grenoble, 85X, 38041 Grenoble Cedex, France

Received 10 April 1992; accepted 9 July 1992

A model is proposed for the crystalline-to-amorphous transformation (amorphization) of $Zr(Cr, Fe)_2$ precipitates in Zircaloy under neutron irradiation. The model is based on the observations that a "duplex" structure forms upon neutron irradiation: an amorphous layer starts at the precipitate–matrix interface that moves into the precipitate until the precipitate is completely amorphous. A depletion of Fe from the amorphous layer is observed, and the thickness of the amorphous layer is directly proportional to fluence. This last feature cannot be accounted for by models in which the rate controlling step for amorphization is diffusion-controlled.

The rate-controlling step for amorphization is a departure from stoichiometry induced by ballistic mixing across the crystallineamorphous interface. This explains the fact that amorphization starts at the interface and gives the correct linear dependence of amorphous layer thickness with fluence. It is shown that the amorphization front velocity observed experimentally can be reproduced with the present model.

1. Introduction

The size and distribution of the intermetallic precipitates $Zr(Cr, Fe)_2$ usually found in Zircaloy-4, have been found to influence in-reactor waterside corrosion rates [1,2]. In that context, dissolution and reprecipitation of those precipitates could be of importance in determining Zircaloy corrosion behavior under irradiation.

$Zr(Cr, Fe)_2$ precipitates undergo a crystalline-to-amorphous transformation (amorphization) and eventually dissolve under neutron irradiation [3,4], after a dose of 1–10 dpa. Partially amorphized precipitates exhibit an amorphous layer at the precipitate–matrix interface that gradually moves into the precipitate, until the whole precipitate is amorphous. A decrease in iron concentration is associated with the transformation. A qualitative model has been proposed by Yang [5] for the crystalline-to-amorphous transformation of those precipitates based on exchanges of vacancies with iron atoms at the precipitate–matrix interface. Some of the shortcomings of this model have been discussed by Griffiths [6], who proposes instead that the Fe interstitials created by irradiation in the intermetallic precipitate are less stable than the ones in the Zr matrix, so they tend to leave the precipitate to go into the matrix, leading to the observed iron depletion. The iron depletion reduces the Fe/Cr ratio in the thin layer of $Zr(Cr, Fe)_2$ closest to the matrix making it less stable against amorphization than the core of the $Zr(Cr, Fe)_2$ precipitate with the normal Fe/Cr ratio of 1.5. In other words, the free energy difference between the crystalline and the amorphous phases of $Zr(Cr, Fe)_2$ decreases with decreasing Fe/Cr ratio.

Besides making no quantitative predictions, these models fail to predict some of the qualitative characteristics of the transformation, notably the fact that diffusion-controlled processes are incompatible with the linear dependence of the amorphous layer thickness on fluence, as will be discussed below. It is the purpose of this article to present a model for amorphization of $Zr(Cr, Fe)_2$ precipitates in Zircaloy under high temperature neutron irradiation that can calculate the velocity of advancement of the amorphous front, while giving the correct dependence on fluence and explaining the amorphization morphology.

[1] Presently at The Pennsylvania State University, Department of Nuclear Engineering, 231 Sackett Building, University Park, PA 16802, USA.

Elsevier Science Publishers B.V.

2. Brief review of experimental results

The intermetallic precipitates $Zr(Cr, Fe)_2$ in Zircaloy have been made amorphous both by charged particle and by neutron irradiation [7]. The results for amorphization under neutron irradiation used in this article have been presented elsewhere in full [8–10], and only a brief review is given here to orient the choice of a theoretical model.

Amorphization is observed in $Zr(Cr, Fe)_2$ precipitates in neutron irradiated Zircaloy-2 and -4. Fig. 1 shows the dose to amorphization of $Zr(Cr, Fe)_2$ precipitates in Zircaloy-4 plotted against temperature. Those results are for a fixed precipitate size since the dose to amorphization depends on the size of the precipitate. At low temperature (around 330 K), the dose to amorphization is < 1 dpa. It increases between 520 and 580 K, up to values of about 10 dpa. Above a critical temperature between 580 and 600 K, no amorphization is observed for practical irradiation conditions. Since the melting temperature of $ZrCr_2$ is 1900 K, the critical temperature corresponds to approximately $0.3T_m$ [11], where T_m is the melting temperature.

As indicated in fig. 1, close to the critical temperature, amorphization starts at the precipitate-matrix interface and gradually moves inwards, until the whole precipitate is amorphous. An intermediary stage is shown in fig. 2. The core of the precipitate is crystalline as evidenced by the stacking faults visible in bright field as well as by the presence of a spot diffraction pattern. The outer layer is amorphous, as shown by the presence of a ring diffraction pattern, and by the fact that the diffraction contrast in bright field does not change as the precipitate is tilted to different orientations. It is found [9] that the increase of amorphous layer thickness in $Zr(Cr, Fe)_2$ precipitates in Zircaloy-4 is linear with fluence throughout the irradiation time before complete amorphization. This is shown in fig. 3 where the amorphous thickness is plotted against fluence. The slope is constant from beginning to end of irradiation time and there is no sign of an incubation period for the formation of the amorphous layer. The slope measured from fig. 3 is equal to 10 nm

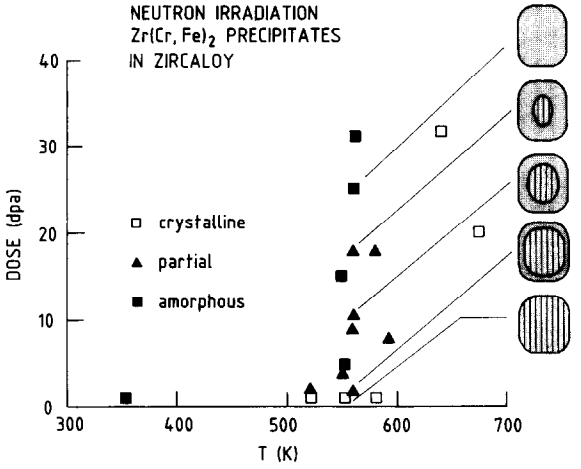

Fig. 1. Dose to amorphization under neutron irradiation of $Zr(Cr, Fe)_2$ precipitates in Zircaloy-4 against temperature. The amorphization process is shown schematically for the points at 580 K: the thickness of the amorphous layer increases with fluence until complete amorphization of the precipitates.

Fig. 2. $Zr(Cr, Fe)_2$ precipitate after irradiation to fluence of 4×10^{25} n m^{-2}, in the BR3 reactor. The amorphous layer (A) formed at the precipitate–matrix interface gradually moves into the crystalline core (C) until the whole precipitate is amorphous. (Courtesy of C. Regnard, CENG-SECC).

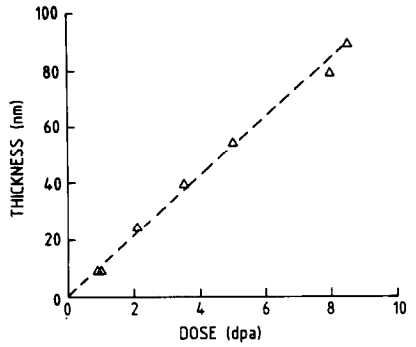

Fig. 3. Amorphous layer thickness in $Zr(Cr, Fe)_2$ precipitate under neutron irradiation at temperatures between 520 and 580 K. The slope of the straight line is about 10 nm/10^{25} n m^{-2} [9,10].

per 10^{25} n m^{-2} in the range of temperature from 523 to 580 K. Some of the fluence data in fig. 3 come from irradiations done at different neutron fluxes for the same time [12], therefore different fluxes give different rates of amorphous layer advancement.

Chemical analysis shows that iron is substantially depleted in the amorphous layer compared to the crystalline precipitate. This can be verified in fig. 4 reproduced from ref. [4]. While the chromium concentration remains constant inside the precipitate, the iron concentration falls steeply across the crystalline/amorphous interface, remains at a lower level in the amorphous layer and falls again abruptly at the precipitate–matrix interface. The iron concentration is 40 at% in the precipitate, and approximately 10 at% in the amorphous layer, falling to close to 0 in the zirconium matrix.

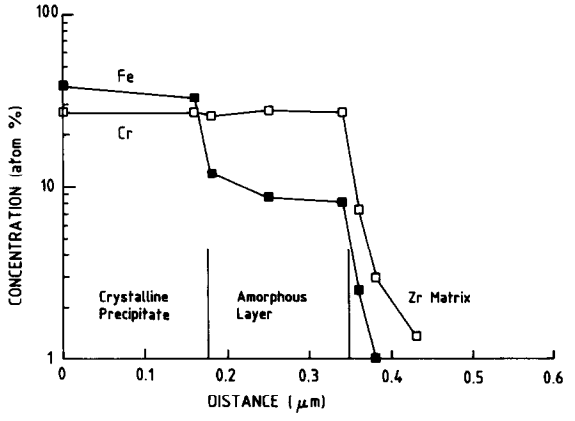

Fig. 4. Iron and chromium concentrations against distance in partially amorphized $Zr(Cr, Fe)_2$ precipitate similar to the one shown in fig. 2, from ref. [4]. The iron content of the amorphous layer is substantially reduced compared to the crystalline core, but is larger than that of the zirconium matrix.

3. Model for neutron-irradiation-induced amorphization

3.1. General observations

The exponential increase of the dose-to-amorphization with temperature indicates that amorphization induced by neutron irradiation close to the critical temperature, T_c, can be interpreted as a competition between irradiation damage and thermal annealing, as observed for other types of irradiation [13–17]. At low temperatures, irradiation damage accumulates in the lattice, unopposed by thermal annealing, until the energy stored is high enough to permit amorphization. This happens between 0.5 and 1 dpa. At higher temperatures thermal annealing processes are activated that reduce the rate of accumulation of irradiation damage, thereby raising the dose to amorphization. Finally, at the critical temperature, the annealing rate becomes faster than the irradiation damage rate and amorphization does not happen. As stated above, the amorphization condition is

$$\Delta G_{irr} > \Delta G_{ca}, \tag{1}$$

where ΔG_{irr} is the increase in free energy brought about by irradiation and ΔG_{ca} is the difference in free energy between the crystalline and amorphous phases. ΔG_{irr} is the sum of the different forms of energy stored by irradiation in the lattice. In addition to the forms of energy storage usually considered, i.e. increase in point defect concentration [13] and chemical disordering [18], the free energy increase from the departure from stoichiometry should also be considered in this case as pointed out in ref. [9].

The increase in free energy under irradiation is then written as

$$\Delta G_{irr} = \Delta G_{st} + \Delta G_{dis} + \Delta G_{def}, \tag{2}$$

where ΔG_{st}, ΔG_{dis} and ΔG_{def} are the changes in free energy due to departure from stoichiometry, chemical disordering and point defect increase, respectively. The change in free energy due to the increase in point defect concentration under irradiation can be neglected here because the steady state point defect concentration under neutron irradiation is very small

at reactor operating temperatures ($C_i \ll C_v < 10^{-6}$, where C_i and C_v are the interstitial and vacancy concentrations, respectively) [19].

In the next sections it is shown that the observed amorphization morphology and kinetics can be explained if the departure from stoichiometry controls the amorphization process.

3.2. Model

The fact that amorphization starts at the precipitate–matrix interface indicates that the matrix plays some role in the amorphization process. That role is probably linked to the iron depletion associated with amorphization. The linear dependence of the amorphous thickness with fluence suggests that the rate-controlling step for advancement of the amorphous front into the crystalline core is not diffusional as proposed elsewhere [5,6], since for a thermal diffusion controlled process, the thickness should be proportional to the square root of the irradiation time, $t^{1/2}$, where it is in fact proportional to ϕt. Furthermore, in the present case, a process controlled by thermal diffusion would imply that all precipitates plotted in fig. 3 would have roughly the same amorphous layer thickness, since they were irradiated for the same amount of time, and at the same temperature, albeit at different dose rates. Since the thickness is actually proportional to the fluence ϕt, it is likely that diffusional processes do not control amorphization. The absence of marked gradients in the iron concentration either in the amorphous layer or in the zirconium matrix and the absence of an incubation period, further argue for a process that is not controlled by diffusion.

The linear dependence of the amorphous thickness on fluence can be explained if amorphization happens at a critical departure from stoichiometry caused by mixing across the interface originating from atomic collisions (ballistic mixing). This is because the amount of ballistic mixing across an interface is proportional to the fluence [20,21].

The model proposed in this work is illustrated in fig. 5. The zone in the precipitate close to the matrix has its iron and chromium sputtered away into the matrix by collisions with neutrons or with knock-on ions produced in neutron-induced cascades. Since intermetallic compounds exist only in a narrow compositional range, their free energy rises steeply with small departures from stoichiometry [16], as illustrated qualitatively in fig. 6. As soon as a critical departure from stoichiometry δc, and thus ΔG, is attained in a given layer, the free energy of the depleted intermetallic layer becomes larger than that of the amorphous phase. When that happens, that layer is unstable with respect to the amorphous phase and amorphization can occur.

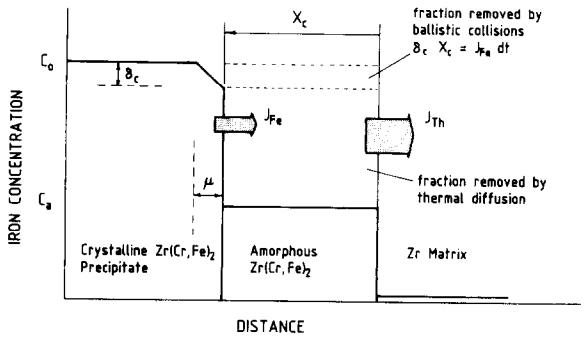

Fig. 5. Model for neutron irradiation induced amorphization: ballistic collisions induce a net flux of iron J_{Fe} across the crystalline/amorphous interface which causes a departure from stoichiometry δc in the thin region μ. This locally raises the free energy and makes that region amorphize preferentially. Once the amorphous transformation occurs, a larger quantity of iron is released from the precipitate into the matrix (J_{th}), due to a new chemical equilibrium.

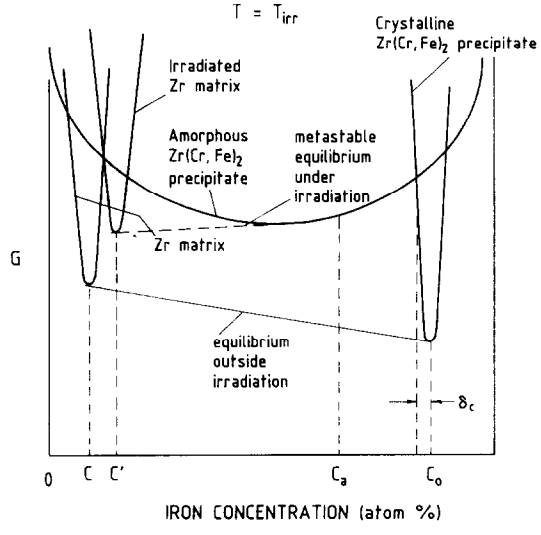

Fig. 6. Schematic free energy curves for the phases present under irradiation. Amorphization changes the equilibrium between matrix and precipitate from the solid to the dotted line. As a consequence, the concentration of iron in the precipitate changes, from C_0 to C_a. A slight increase in iron solubility from C to C', due to the higher point defect concentration under irradiation, can also contribute to Fe depletion.

Once the transformation takes place, a much larger variation in concentration happens as the amorphous phase discharges its iron into the zirconium matrix in order to attain the new equilibrium concentration C_a.

The justification for the iron discharge after amorphization is that the equilibrium iron concentration between the amorphous precipitate and the irradiated zirconium matrix is different from that between the crystalline precipitate and the unirradiated zirconium matrix. That there can be a change in the equilibrium iron concentration is shown schematically in fig. 6. The equilibrium between the intermetallic precipitate and the zirconium matrix that exists before irradiation is represented by the full line. After amorphization a new metastable equilibrium exists between the amorphous phase and the irradiated zirconium matrix (dotted line). At this new "pseudoequilibrium", the iron concentration in the amorphous precipitate C_a is lower than $C_0 - \delta c$, the composition at which the amorphous phase is formed, so in order to attain the new equilibrium, iron is depleted into the matrix. This is helped by the effective increase in iron solubility in the matrix caused by the supersaturation of point defects present under irradiation. This is shown qualitatively in fig. 6: irradiation shifts the minimum in the zirconium matrix free energy curve from C to the higher C'. Both of these factors can lead to iron depletion from the amorphous phase into the matrix. If the thermal diffusion steps are fast compared to the ballistic jump across the crystalline–amorphous interface, then the iron concentration profiles in the amorphous layer and in the matrix should be flat as observed in fig. 4.

Indeed there is some evidence that most of the observed variation in iron concentration happens after amorphization and not vice versa. Intermetallic precipitates in Zircaloy made amorphous by low temperature ion irradiation do not change their composition upon amorphization [24]. However, there are preliminary indications that they discharge some of their iron into the matrix upon postamorphization heat treatment below the recrystallization temperature [25]. Heat treatment at 675 K for three days decreases the Fe/Cr ratio at the precipitate edges from 1.7 to 1.5, while heat treatment at 775 K for three days decreases the overall Fe/Cr ratio in the precipitate from 1.7 to between 1.4 and 1.0. Those results indicate that, after amorphization, iron spontaneously leaves the precipitate, not even necessitating the higher effective solubility under irradiation.

Fig. 4 shows that there is little variation in the chromium concentration from the crystalline precipitate to the amorphous layer. The reason why chromium atoms are not discharged into the matrix along with the iron atoms is probably kinetic: the chromium diffusion coefficient in pure alpha-zirconium is much smaller than the corresponding diffusion coefficient of iron: at 600 K D_{Zr}^{Fe} is about 10^{-12} m^2 s^{-1}, while D_{Zr}^{Cr} is of the order of 10^{-18} m^2 s^{-1} [22].

The process is summarized as follows: first an amorphous layer is formed at the precipitate–matrix interface because of a small variation in the (Fe + Cr) concentration in the precipitate, caused by ballistic sputtering of those atoms into the Zr matrix. Once the amorphous phase is formed, there is a discharge of iron from the amorphous phase into the matrix, until an "equilibrium" concentration C_a is reached. The layer continues to advance, by a ballistically-induced depletion of iron atoms from the crystalline to the amorphous part of the precipitate followed by a fast discharge into the matrix after amorphization. Since there is no thermally-induced discharge of chromium to the amorphous layer and then to the zirconium matrix, the amount of chromium on both sides of the crystalline–amorphous interface is approximately equal, so mixing across the boundary has a smaller effect. The actual depletion of chromium in the thin layer is then small compared with that for iron.

The conditions for the above scheme to be valid are

$$D_{Fe}^{Zr},\ D_{Fe}^{am} \gg D_{Fe}^{bal} \gg D_{Fe}^{pt}, \tag{3}$$

where D_{Fe}^{Zr} is the iron diffusion coefficient in the zirconium matrix, D_{Fe}^{am} is the iron diffusion coefficient in the amorphous Zr–Cr–Fe phase, D_{Fe}^{bal} is the ballistic diffusion coefficient and D_{Fe}^{pt} is the iron diffusion coefficient in the crystalline intermetallic precipitate $Zr(Cr, Fe)_2$. When the conditions in eq. (3) are satisfied, the rate controlling step of the process is ballistic rather than thermal diffusion.

D_{Fe}^{bal}, can be estimated from

$$D_{Fe}^{bal} = \tfrac{1}{6}\Gamma\langle x\rangle^2, \tag{4}$$

where the ballistic jump frequency Γ is equal to the displacement rate $\phi\sigma_d$, (with σ_d the displacement cross section), and $\langle x\rangle$ is the average distance travelled by an atom in a collision. The displacement cross section used here is the classical value that does not take into account the production of free defects. Taking a displacement rate $\phi\sigma_d$ of 5×10^{-7} dpa s^{-1}, typical of neutron irradiation, and an $\langle x\rangle$ of 5 nm as an upper limit of the average distance travelled by an atom in a neutron collision cascade, we obtain $D_{Fe}^{bal} = 2 \times 10^{-24}$ m^2 s^{-1}. The thermal diffusion of iron is dependent of alloy composition: in pure zirconium it is of the order of 5×10^{-13} m^2 s^{-1} at 560 K [22], while in alloys like

Zircaloy and Zr–Nb by extrapolation of the high temperature data it would be in the range of 10^{-18} m^2 s^{-1} at 580 K [26].

Even though not much is known about D_{Fe}^{pt}, it is reasonable to suppose that it is smaller than D_{Fe}^{Zr}. This is because iron has been shown to be a very fast interstitial diffuser in zirconium [22], while in the ordered intermetallic compound it is likely that the iron interstitial configuration is a complicated one involving several atoms in order to minimize local disorder, analogously to what is observed in molecular dynamics simulations of other intermetallic compounds [27,28]. This leads to a high interstitial migration energy [27]. Taking the preexponential factor for iron diffusion in the intermetallic to be $D_0 = 10^{-6}$ m^2 s^{-1}, the migration energy of iron in the intermetallic needs to be higher than 2 eV, a condition expected to be fullfilled, in order for the condition expressed in eq. (3) ($D_{Fe}^{bal} \gg D_{Fe}^{pt}$) to be satisfied at the irradiation temperature of 580 K.

The diffusion of Fe in amorphous $Fe_{24}Zr_{75}$ alloy has been observed to be high [29] and the values reported for D_0 and the activation energy outside of irradiation corresponds to $D_{Fe}^{am} = 6.2 \times 10^{-21}$ m^2 s^{-1} at 580 K, again fullfiling condition (3).

The model is now used to calculate the velocity of advancement of the amorphous front.

3.3. Calculation of the amorphous front velocity

Assuming the planar geometry shown in fig. 5 the flux of atoms sputtered across the interface from the crystalline to the amorphous part of the precipitate is [30]

$$J_+ = \tfrac{1}{2}\int_0^{\mu} C(x)\phi\sigma_d(1 - x/\mu)\,dx, \tag{5}$$

where μ is the average range of the sputtered atoms, and $C(x)$ is the iron concentration profile in the intermetallic precipitate as a function of the distance from the crystalline–amorphous interface, x. Since the sputtering probability decreases linearly with x, and using the boundary conditions $C(\mu) = C_0$ and $C(0) = C_0 - \delta c$, where C_0 is the concentration of iron in the original intermetallic precipitate particle, then

$$C(x) = C_0 - (1 - x/\mu)\,\delta c. \tag{6}$$

Substituting eq. (6) into eq. (5) and performing the integration yields

$$J_+ = \tfrac{1}{4}\mu\phi\sigma_d\left(C_0 - \tfrac{2}{3}\,\delta c\right). \tag{7}$$

This is the flux from the crystalline core to the amorphous layer. The reverse flux is

$$J_- = -\tfrac{1}{4}\mu\phi\sigma_d C_a. \tag{8}$$

Then the total flux across the crystalline–amorphous interface is

$$J_{Fe} = J_+ + J_- = \tfrac{1}{4}\mu\phi\sigma_d\left(C_0 - C_a - \tfrac{2}{3}\,\delta c\right). \tag{9}$$

Since, according to the model, the flux J_{Fe} is responsible for the iron depletion leading to amorphization, the total amount of iron sputtered per unit area of precipitate–matrix interface after time t is equal to the thickness of the amorphous layer multiplied by the critical change in concentration δc, or

$$J_{Fe}t = X_c(t)\,\delta c, \tag{10}$$

where $X_c(t)$ is the thickness at time t of the layer that has amorphized due to having reached the critical departure from stoichiometry for amorphization. Substituting eq. (9) into eq. (10) and solving for X_c we obtain

$$X_c(t) = \tfrac{1}{6}\mu\phi\sigma_d t\left[\tfrac{3}{2}(C_0 - C_a)/\delta c - 1\right]. \tag{11}$$

It can be seen from eq. (11) that X_c is proportional to the fluence ϕt as observed experimentally. Using $\phi\sigma_d = 5 \times 10^{-7}$ dpa s^{-1}, $C_0 = 0.4$ and $C_a = 0.1$, we find that δc needs to be 3 at% for the calculated value of the amorphous layer advancement X_c to correspond to the experimental value of 10 nm/10^{25} n m^{-2}.

3.4. Evaluation of ΔG_{st}

One possible check to the model is to independently evaluate ΔG_{st} and verify that the value of δc calculated above provides the correct order of magnitude of free energy variation to induce amorphization, that is, to check that ΔG_{st} originating from a 3% variation in stoichiometry is comparable to ΔG_{ca}. It is necessary then, to estimate by how much the free energy varies when there is a departure from stoichiometry. This depends mainly on the type of defect formed, point defect or anti-site. Only the anti-site defects are considered here, that is, it is assumed that the mixing occurs by the reaction

$$Zr^m + Fe^p \rightleftharpoons Zr^p + Fe^m, \tag{12}$$

where Zr^m is a zirconium atom in the matrix, Fe^p is an iron atom in the precipitate and the others are similar. Then a zeroth order approximation is to take

$$\Delta G_{st} = \Delta H_{st} - T\,\Delta S_{st} = Z\Omega\,\delta c + RT[\delta c\,\ln\,\delta c + (1 - \delta c)\,\ln(1 - \delta c)], \tag{13}$$

where Z is the number of iron nearest neighbors to a zirconium-type site and Ω is the ordering energy. The departure from stoichiometry δc is equal to the concentration of iron in the zirconium sites of the intermetallic compound. When the departure from stoichiometry is small enough that the entropic contribution is not important, the form of ΔG_{st} given by eq. (13) is of a linear variation with the departure from stoichiometry. More realistically, ΔG_{st} should increase as $(\delta c)^2$, so the approximation above underestimates ΔG_{st}.

Using $Z = 8$, $\Omega = 0.03$ to 0.01 eV [31] and a variation in iron concentration of 3%, we obtain a value of $\Delta G_{st} = 0.004$ to 0.013 eV per atom, which represents 20 to 65% of the difference in free energy between the crystalline and amorphous phases, about 0.02 eV per atom [32].

Therefore according to the preceding calculation, a departure from stoichiometry in line compounds can store enough energy in the lattice to cause an amorphous front to form preferentially at the crystalline–amorphous interface and to drive it into the crystalline core at the velocity observed experimentally.

4. Discussion

The model presented in the preceding section rationalizes the linear dependence of the amorphous thickness on fluence, the absence of an incubation period and the preferential amorphization at the precipitate boundaries. The proposition of amorphization by departure from stoichiometry is analogous to the situations of amorphization at metallic layer interfaces by diffusion couples [33] or by ion mixing [34]. In both of those cases the off-stoichiometric mixing of two metallic layers (in one case by collisional mixing in the other by a fast diffuser), creates an amorphous layer, due to the difficulty in forming the more energetically favorable intermetallic phase [35,36]. The difference here is that the energetically most favorable configuration (a two-phase mixture of Zr matrix and $Zr(Cr, Fe)_2$ precipitates) already exists from the beginning and is destabilized by a departure from stoichiometry caused by irradiation. This creates the conditions for the amorphous layer to appear at the interface.

Several works in the literature have indicated that chemical disordering is a major driving force for amorphization of intermetallic compounds under irradiation, both in experiments [18,29] and in molecular dynamic (MD) simulations [37], although there is evidence that point defects also play an important role [38,39]. In the present work, a contribution by homogeneous chemical disordering in the precipitate to the general free energy increase of the intermetallic phase during irradiation has been ruled out because of the twin considerations of linear kinetics and the absence of buildup time, as explained in the following.

Chemical disordering by statistical processes gives not a linear but an exponential dependence of the long range order parameter S on fluence [40]. The dependence of ΔG_{dis} on S is given by the Bragg–Williams model, in the absence of thermal reordering as $(1 - S^2) = (1 - e^{-2\phi t})$ [17], Since the thermal reordering term is a complex function of S, the ordering energy, and of the temperature, but completely independent of fluence, this means that linear kinetics would not be observed if bulk chemical disordering were the controlling mechanism. In addition, since there is no incubation time, the amount of homogeneous chemical disordering that is compatible with linear kinetics is a steady state of very low disorder that is quickly attained, leading to a small contribution from bulk disordering to the free energy rise under irradiation. It is possible that chemical disordering brought about by cascades contributes locally to the increase in free energy. However, because amorphization starts at the precipitate–matrix interface, the rate-controlling mechanism for amorphization is thought to be a departure from stoichiometry.

With this model, it is interesting to consider what annealing mechanism precludes amorphization from occurring when the material is irradiated above the critical temperature T_c.

On the one hand, it is possible that at the critical temperature the condition $D_{Fe}^{pt} \ll D_{Fe}^{bal}$ expressed in eq. (3) ceases to be valid. In that last case, any small departure from stoichiometry is quickly evened out through the whole intermetallic compound, and the critical departure from stoichiometry is not reached. Alternatively, it is possible that at $T = T_c$, ΔG_{dis} is substantially reduced due to a cascade annealing process being activated.

The temperature of $0.3T_m$ has been shown [20] to be the temperature at which the thermally assisted regime becomes important with respect to ballistic processes during cascade annealing, both for direct amorphization and for cascade mixing. The fact that the critical temperature corresponds very nearly to $0.3T_m$ supports the second explanation. In that case, depletion would still occur, but the level of damage necessary for amorphization would not be reached due to the absence of cascade damage. Some precipitate

dissolution under irradiation above T_c has been observed [9], supporting the scheme above.

It is important to note that the amorphization model described here is not applicable to low temperature irradiation, where the iron diffusion coefficients in the zirconium matrix and in the amorphous layer are too low. There are indications that the neutron irradiation induced amorphization process at low temperature (330 K) is qualitatively different from that at high temperature (550 K): one, it happens without any change in stoichiometry and, two, the crystallization temperatures upon postirradiation annealing are different for precipitates amorphized at low and high temperature [9]. This is another example of a system where the amorphization mechanisms at high and low temperature are different, analogously to those mentioned in ref. [31].

The importance on the zirconium matrix to the current process indicates that the amorphization process induced by irradiation depends not only on the behavior of the precipitate itself but on that of the whole system. Amorphization also depends on the nature of the irradiating particle [7]. It is recalled here that under 1.5 MeV electron irradiation, amorphization of $Zr(Cr, Fe)_2$ precipitates takes place only below 300 K, without changes in precipitate stoichiometry and in a spatially homogeneous fashion [41]. In that case, it is believed that both the contributions of point defect supersaturation and chemical disordering contribute to amorphization.

Under ion irradiation, the transformation also takes place without change in stoichiometry [23]. This transformation was tentatively attributed to chemical disordering caused by cascades [7,17].

The dynamic role played by ballistic mixing in this case indicates the importance of taking into account not only thermodynamical considerations of phase stability, but the competing kinetics of thermal and ballistic processes as well when modelling the crystalline–amorphous transformation under irradiation.

5. Conclusions

The model presented here explains some of the characteristics of the crystalline to amorphous transformation of $Zr(Cr, Fe)_2$ precipitates in Zircaloy under neutron irradiation at power reactor temperatures.

According to this model, amorphization happens by a departure from stoichiometry due to a ballistic interchange of iron and zirconium atoms across the precipitate–matrix interface. This explains the observation that amorphization starts at the precipitate matrix interface forming a front that gradually moves into the precipitate. It also agrees with the observed kinetics of amorphization, predicting an amorphous thickness proportional to fluence and the absence of an incubation period for the transformation to start.

This model is valid at high temperatures and has specific requirements of relative magnitudes of diffusion coefficients to work. Using the model, the velocity of the amorphous front is calculated, and it is found that a depletion of about 3% in the iron concentration reproduces the observed velocity.

Acknowledgements

Stimulating discussions with P Desré, M. Griffiths, R.A. Holt and F. Rossi are gratefully acknowledged.

Part of this work his work was done while one of the authors (ATM) was at AECL/Chalk River Laboratories and was supported in part by the Candu Owners Group (COG).

References

[1] F. Garzarolli and H. Stehle, IAEA Int. Symp. on Water Reactor Technology, Stockholm, September 1986, IAEA SM-288-24.
[2] D.G. Franklin and P.M. Lang, Proc. 9th Int. Symp. on Zirconium in the Nuclear Industry, Kobe, Japan, November 1990, ASTM-STP 1132 (1991) 3.
[3] R.W. Gilbert, M. Griffiths and G.J.C. Carpenter, J. Nucl. Mater. 135 (1985) 265.
[4] W.J.S. Yang, R.P. Tucker, B. Cheng and R.B. Adamson, J. Nucl. Mater. 138 (1986) 185.
[5] W.J.S. Yang, J. Nucl. Mater. 158 (1988) 71.
[6] M. Griffiths, J. Nucl. Mater. 170 (1990) 294.
[7] A.T. Motta, F. Lefebvre and C. Lemaignan, Proc. 9th Int. Symp. on Zirconium in the Nuclear Industry, Kobe, Japán, November 1990, ASTM-STP 1132 (1991) 718.
[8] M. Griffiths, J. Nucl. Mater. 159 (1988) 190.
[9] M. Griffiths, R.W. Gilbert and G.J.C. Carpenter, J. Nucl. Mater. 150 (1987) 53.
[10] W.J.S. Yang, EPRI report NP-5591 (1988).
[11] D. Arias, J.P. Abriata, Bull. Alloy Phase Diagr. 7 (1986) 237.
[12] M. Griffiths, personal communication.
[13] M.L. Swanson, J.R. Parsons and C.W. Hoelke, Radiat. Eff. 9 (1971) 249.
[14] K.C. Russell, Prog. Mater. Sci. 28 (1984) 229.
[15] K.Y. Liou and P. Wilkes, J. Nucl. Mater. 87 (1979) 317.
[16] M. Nastasi and J.W. Mayer, Mater. Sci. Rep. 6 (1991) 1.
[17] A.T. Motta and D.R. Olander, Acta Metall. Mater. 38 (1990) 2175.

[18] D.E. Luzzi and M. Meshii, Res. Mechanica 21 (1987) 207.
[19] H. Wiedersich, Radiat. Eff. 12 (1972) 111.
[20] F. Rossi and M. Nastasi, J. Appl. Phys. 69 (1991) 1310.
[21] W.L. Johnson, Y.T. Cheng, M. Van Rossum and M.-A. Nicolet, Nucl. Instr. and Meth. B7/8 (1985) 657.
[22] G. Hood, J. Nucl. Mater. 159 (1988) 149.
[23] F. Lefebvre and C. Lemaignan, Proc. AIEA Techn. Comm. Mtg. on Fundamental Aspects of Corrosion of Zr-based Alloys in Water Reactor Environments, Portland, Oregon, September 1989, IWG-FPT/34, pp. 80–88.
[24] F. Lefebvre and C. Lemaignan, J. Nucl. Mater. 165 (1989) 122.
[25] D. Pêcheur, F. Lefebvre, A.T. Motta, C. Lemaignan and J.F. Wadier, J. Nucl. Mater. 189 (1992) 318.
[26] G. Hood and R.J. Schultz, Proc. 8th Int. Symp. on Zirconium in the Nuclear Industry, ASTM-STP 1023 (1989) 435.
[27] J.R. Schoemaker, R.T. Lutton, D. Wesley, W.R. Wharton, M.L. Oehrli, M.S. Herte, M.J. Sabochik and N.Q. Lam, J. Mater. Res. 6 (1991) 473.
[28] A. Caro, M. Victoria and R.S. Averback, J. Mater. Res. 5 (1990) 1409.
[29] J. Horvath, F. Ott, K. Pfahler and W. Ulfert, Mater. Sci. Eng. 97 (1988) 409.
[30] D.R. Olander, Fundamental Aspects of Nuclear Reactor Fuel Elements, TID 26711-P1, chapter 15, p. 292.
[31] P.R. Okamoto, M. Meshii, in: Science of Advanced Materials, eds. H. Wiedersich and M. Meshii (ASM, 1992) pp. 33–98.
[32] M.P. Henaff, C. Colinet, A. Pasturel, K.H.J. Buschow, J. Appl. Phys. 56 (1984) 307.
[33] J.C. Barbour, R. de Reus, A.W. Denier van den Gon and F.W. Saris, J. Mater. Res. 2 (1987) 168.
[34] L.E. Rehn and P.R. Okamoto, Nucl. Instr. and Meth. B39 (1989) 104.
[35] U. Gosele and K.N. Tu, J. Appl. Phys. 66 (1989) 6.
[36] P.J. Desre and A.R. Yavari, Phys. Rev. Lett. 64 (1990) 13.
[37] C. Massobrio, V. Pontikis and G. Martin, Phys. Rev. B41 (1990) 10486.
[38] A.T. Motta and C. Lemaignan, Proc. European Workshop on Ordering and Disordering in Alloys, Grenoble, France, July 1990, ed. A.R. Yavari (Elsevier, London, 1992) p. 225.
[39] M.J. Sabochik and N.Q. Lam, Scripta Metall. Mater. 24 (1990) 565.
[40] L.R. Aronin, J. Appl. Phys. 25 (1954) 344.
[41] A.T. Motta, D.R. Olander and A.J. Machiels, Proc. 14th Int. Symp. on The Effects of Irradiation on Materials, Andover, ASTM-STP 1046 (1988) 457.